Neonatal White Matter Damage Analysis using DTI Interpolation and Multi-modality Image Registration.

Yi Wang[a,*], Yuan Zhang[a], Chi Ma[a], Yu Shen[b], Rui Wang[a], Zhe Guo[a] and Hongying Meng[c]

[a]School of Electronics and Informatio, Northwestern Polytechnical University, Shaanxi, CHINA
[b]Henan Provincial People's Hospital, Zhengzhou, CHINA
[c]College of Engineering, Design and Physical Sciences, Brunel University London, UK

ARTICLE INFO

Keywords:
Diffusion Tensor Magnetic Resonance Imaging
T1 MRI
Punctate White Matter Damage
Fiber Tractography
Tensor Super-Resolution

ABSTRACT

Punctate White Matter Damage (PWMD) is a common neonatal brain disease. Especially, at the neonatal stage, the best cure time can be easily missed because PWMD is not conducive to the diagnosis based on current existing methods. Diffusion Tensor Magnetic Resonance Imaging (DT-MRI, shorted as DTI) is a non-invasive technique that can study brain microstructures in vivo, and provide information on movement and cognition-related fiber tracts and the lesion of PWMD is relatively straightforward on T1 MRI, showing the center of the semi-oval, lateral ventricle, cluster, or linear T1 high signals. Therefore, we ppropose a new pipeline to use T1 MRI combined with DTI for better neonatal PWMD analysis based on DTI interpolation and multi-modality image registration. Firstly, after preprocessing, neonatal DTI super-resolution is performed with the three times B-spline interpolation algorithm based on the Log-Euclidean space to improve DTIs' resolution to fit the T1 MRIs and facilitate fiber tractography. Secondly, the Symmetric Diffeomorphic registration algorithm and inverse b0 image were selected for multi-modality image registration of DTI and T1 MRI. Finally, the 3D lesion models were combined with fiber tractography results to analyze and predict the degree of PWMD lesions affecting fiber tracts. Extensive experiments demonstrated the effectiveness and super performance of our proposed method in comparison with alternative methods. This streamlined technique plays an essential auxiliary role in diagnosing and treating neonatal PWMD.

1. Introduction

Punctate White Matter Damage (PWMD) is one of the most common white matter damages in preterm infants (Niwa et al., 2011; Nguyen et al., 2019; Tusor et al., 2017). 22% of premature infants show PWMD, and the symptoms are cognitive, motor or a visual impairment, and even develop into cerebral palsy in the later stages(Arrigoni et al., 2016). These symptoms are not evident in the neonatal period, so the best treatment period is easily missed. Therefore, converting undetectable clinical signs into quantifiable results to analyze and predict PWMD by related medical image processing methods is crucial for disease treatment and neurodevelopment.

The lesion of PWMD is relatively clear on T1 MRI, showing the center of the semi-oval, lateral ventricle, cluster, or linear T1 high signals (Wang & Mao, 2014). Meanwhile, the cerebral white matter fiber tracts from Diffusion Tensor Magnetic Resonance Imaging (DT-MRI, referred to as DTI) can be related to movement and cognition. The status of neonatal PWMD can be analyzed and predicted by the damage to white matter fiber tracts. Therefore, the image fusion technique of DTI and T1 MRI is used to research and analyze neonatal PWMD, combining the DTI tractography results with the lesions in T1 MRI. However, because the collection of neonatal DTI is more complex, the resolution is much lower than the T1 MRI, which is not conducive to the registration with the T1 MRI. And the DTI tractography results are not precise enough because the development of neonatal fiber tracts is incomplete. To solve the abovementioned problems, the image super-resolution technique is used for DTI to improve the resolution and the tractography results.

Moreover, the fusion of DTI and T1 MRI is usually performed by image registration. But there are few methods of this multi-modality image registration since DTI is a tensor image, while T1 MRI is a scalar image. Therefore, a new pipeline of neonatal PWMD analysis based on DTI super-resolution and multi-modality image registration is proposed.

DTI super-resolution algorithms can be divided into two categories. The first is the traditional tensor interpolation algorithm, and the other is the super-resolution method based on learning. Different from general scalar image interpolation, the tensor interpolation of DTI is much more complicated. Several tensor interpolation methods have been proposed. For example, tensor interpolation method based on tensor component form (Zhukov & Barr, 2002), improved bilinear tensor interpolation method based on image gradient features of the tensor field (B, 2007) , and tensor interpolation method based on tensor eigenvalues and eigenvectors. These Euclidean space tensor interpolation methods can be calculated, but the swelling and non-positive definite effects of the interpolated tensor may be caused (Hotz et al., 2010; Yassine, 2010). The tensor interpolation method based on Riemann space (Pennec et al., 2006) can avoid these defects, but the calculation is too complicated and takes a long time. In recent years, the development of super-resolution methods based on learning has been proposed more and

*Corresponding author.
E-mail addresses: wangyi79@nwpu.edu.cn (Y. Wang)
ORCID(s): 0000-0002-7743-1779 (Y. Wang)

more rapidly (Dong et al., 2014; Ledig et al., 2017; Lim et al., 2017; Haris et al., 2018; Bashir & Wang, 2021b; Wang et al., 2022; Bashir & Wang, 2021a); a systematic review of image super-resolution techniques is performed by Bashir et al. (Bashir et al., 2021). This kind of method has a good effect on general images. However, directly applying these networks to DTI tensors will also quickly cause the defects described above and cannot guarantee the consistency and the directions of the tensors. At the same time, the network's training model needs a large amount of data, which is hardly obtained.

The tensor interpolation method based on Log-Euclidean space is a reasonable extension of the Riemann space interpolation method (Arsigny et al., 2006; Arsigny, 2004). In Riemann space, the cone of a positive definite symmetric matrix is regarded as a standard and complete manifold; the swelling effect and non-positive substantial effect can be overcome on this manifold, but the calculation is extensive [14]. In 2006, based on Riemann's space theory, Arsigny et al. (Arsigny et al., 2006; Arsigny, 2004), proposed DTI interpolation in Log-Euclidean space, which can also guarantee the constraint property of tensor and simplify the calculation in Riemannian space. In 2008, Fillard et al. (Fillard, 2008) proposed a linear interpolation method based on Riemannian space. However, the interpolation process will damage the tensor anisotropy (Kung et al., 2011) . Therefore, since the tensor interpolation method based on Log-Euclidean space not only inherits the advantages of the Riemann space tensor interpolation algorithm but also significantly reduces the computational complexity, the B-spline tensor interpolation method based on Log-Euclidean space is chosen in this paper to eliminate swelling effect and non-positive definite effect and also reduced computing time and complexity.

For the registration of DTI and T1 MRI, several registration methods of DTI and T1 MRI have been proposed. For example, Symmetric Dieomorphic (referred to as Syn) Registration of DTI, T1 MRI, and Cerebral Blood Flow MRI (referred to as CBF) (Avants et al., 2007), and the registration of DTI and T1 MRI based on Mutual Information (referred to as MI), which uses DTI as the constraint condition of T1 image in deformation tensor morphometry (Studholme, 2007). For other multi-modality image registration algorithms, there are DTI multi-channel image registration algorithms based on diffeomorphic demons registration (referred to as demons) (Tang et al., 2013), the registration algorithm of DTI and fMRI based on Large Deformation Diffeomorphic Metric Mapping (referred to as LDDMM) (Miller et al., 2005), utilizing convolutional neural networks for medical image registration (Sloan et al., 2018). However, a convolutional neural network needs many image data as the training set. This paper's data set is too small to use a convolutional neural network as the registration method.

Meanwhile, these registration algorithms use FA images for image registration instead of other derivative images of DTI. Therefore, to compare which modality of DTI derivative image is better for the registration with T1 MRI, five derivative images of DTI (including FA, MD, MD-in, b0, b0-in) are tested in this paper. The best derivative image b0-in of DTI is selected as the multi-modality image registration algorithm needed.

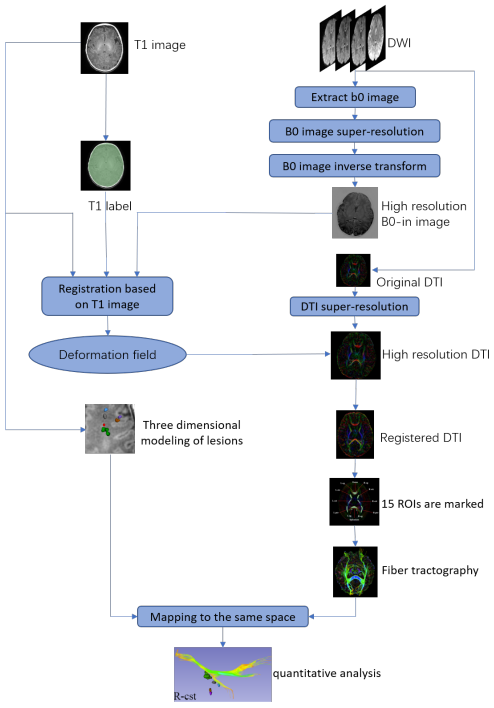

Figure 1: Flowchart of the experiment. First, we use the b0 inverse image with the same resolution to register with the T1 image to obtain the deformation field, which acts on the high-resolution DTI image, and carries out fiber tractography on the DTI image; Then, 3D modeling of lesions reconstruction of T1 image was performed; Finally, the fibers and the lesions were mapped to the same space for quantitative analysis.

In summary, a new pipeline of neonatal PWMD analysis based on DTI super-resolution and multi-modality image registration is proposed in this paper. PWMD can be effectively analyzed in this way.

2. Method

The B-spline tensor interpolation method based on Log-Euclidean space for DTI super-resolution. The DTI and Syn registration algorithm's derivative images are used for DTI and T1 MRI registration. After interpolation and registration, draw 15 ROIs on DTI and used for DTI tractography. The lesions in T1 MRI were modeled in 3D and superimposed with DTI tractography results. The main flowchart is shown in Fig. 1.

2.1. Materials

The neonatal DTI and T1 MRI data are from the Department of Radiology in the First Affiliated Hospital of Xi'an Jiaotong University. A GE 3.0T SignaHDxt MRI scanner was used to scan six neonatal suspected of having PWMD. DTI data is in good shape, and there is no motion artifact. The specific scanning parameters of the DTI data are as follows: 30 gradient directions, b value, is 0 and 600s/mm^2,

TR=11000ms, TE=69.5ms, the layer thickness is 2.5mm, continuous scanning without gaps, FOV=180×180mm, the matrix is 128×128. The DTI resolution is 256×256×44, and the T1 MRI resolution is 256×256×108.

2.2. Pre-processing

In data preprocessing, the diffusion-weighted magnetic resonance images (referred to as DWIs) are performed with the correction of gradient field inconsistency and eddy current. After this, the skull is stripped, and the brain mask is calculated. These steps are completed in FSL (https://fsl.fmrib.ox.ac.uk/fsl/fslwiki/) with default parameters. Finally, tensor estimation is performed in DTI-TK (http://dti-tk.sourceforge.net/pmwiki/pmwiki.php) to obtain the DTI.

2.3. DTI interpolation

Currently, widely used DTI interpolation algorithms are based on Euclidean space, which causes the swelling effect and non-positive definite effect of the interpolation tensor (Dong et al., 2014; Ledig et al., 2017). Non-positive actual effect: after interpolation, the eigenvalue of the interpolated tensor matrix may be zero or negative, which does not meet the requirement of positive-definite of the matrix. This effect will make it challenging to visualize tensor fields. Non-positive definite tensor also has no real physical meaning in image processing. Swelling effect: in the Euclidean space, the interpolated tensor matric, calculated by the weighted sum of two tensors, always has a larger matrix determinant than another tensor matrix. The swelling effect means that the dispersion of random variables corresponding to the interpolation tensor is larger than that of another tensor which is intuitively incompatible with physical meaning.

2.3.1. DTI interpolation based on Riemann space

Fillard (Fillard, 2008) and Pennec (Pennec et al., 2006) proposed a new metric that endows the tensor space with affine-invariant Riemannian metrics to overcome this deficiency. It leads to strong theoretical properties: the positive definite symmetric matrices cone is replaced by a regular and complete manifold without boundaries (null eigenvalues are at infinity). In this metric, the interpolation tensor between two tensors is obtained by its linear interpolation on the shortest geodesic. For affine invariant metrics, the distance between a symmetric matrix with negative eigenvalues and zero eigenvalues and any tensor is infinite. Therefore, this method can avoid the appearance of non-positive eigenvalues. Although the swelling effect and non-positive definite effect are avoided, the amount of interpolation calculation required is much more than other methods.

2.3.2. DTI interpolation based on Log-Euclidean space

Arsigny et al. (Arsigny et al., 2006) proposed a Log-Euclidean space for tensor interpolation to overcome the computational constraints in Riemann space, Arsigny. This method transforms all the computation of tensor matrix into the calculation of vector without any unnecessary complexity and dramatically reduces the computation. And it also can avoid the swelling effect and non-positive definite effect. It is one of the most classical metrics in tensor computing.

2.3.3. B-spline DTI interpolation based on Log-Euclidean space

With the research of affine invariant metrics in Riemann space and Log-Euclidean space, more and more interpolation methods can be used for DTI interpolation. Barmpoutis et al. (Barmpoutis et al., 2007) extended the interpolation method of B-spline in vector value image to tensor image interpolation and proposed B-spline interpolation of tensor image based on Riemann metric.

Suppose there are N diffusion tensors on a one-dimensional grid $(\mathbf{D}_1, \mathbf{D}_2, ...\mathbf{D}_N)$ and then interpolate between these N tensors. In linear interpolation, the interpolated point can be simply computed by a point on a geodesic connecting two continuous tensors can be obtained by computing the points on a geodesic connecting two continuous tensors. In higher dimensional space, a series of control points and node vectors are needed for interpolation. For B-spline interpolation in k-1 times tensor space, there should be $N + k - 2$ control points $(\mathbf{A}_0, \mathbf{A}_1, ...\mathbf{A}_{N+k-3})$ and $N + 2(k-1)$ nodes $(\mathbf{B}_{-k+1}, \mathbf{B}_{-k+1}, ..., \mathbf{B}_{N+k-2})$. For tensor $\mathbf{D}(u)$, $u \in [u_j, u_{j+1})$, B-spline interpolation based on Log- Euclidean space are chosen for DTI interpolation. B-spline curve equation in Log-Euclidean space is given by

$$\mathbf{D}(u) = \sum_{j=0}^{n} \widetilde{\mathbf{A}}_j B_{j,k}(u) \tag{1}$$

$\widetilde{\mathbf{A}}_j$ represents the control point tensor in Log-Euclidean space. In this space, cubic B-spline is chosen for DTI interpolation because cubic B-spline is precise enough and has moderate computation. According to the properties of the b-spline curve, the cubic b-spline ($k = 3$) curve equation of tensor in Log-Euclidean space is given by

$$\mathrm{D(u)}{=}\exp\left(\frac{1}{6}\begin{pmatrix}u^3 & u^2 & u^1 & 1\end{pmatrix}\mathbf{M}_\alpha\begin{pmatrix}\log(\mathbf{D}_0)\\ \log(\mathbf{D}_1)\\ \log(\mathbf{D}_2)\\ \log(\mathbf{D}_3)\end{pmatrix}\right) \tag{2}$$

$$\mathbf{M}_\alpha = \begin{pmatrix}-1 & 3 & -3 & 1\\ 3 & -6 & 3 & 0\\ -3 & 0 & 3 & 0\\ 1 & 4 & 1 & 0\end{pmatrix} \tag{3}$$

The B-spline curve in Log-Euclidean space is extended to the B-spline surface, and the B-spline surface equation of the two-dimensional tensor space is given by

$$\mathbf{D}(u,v) = exp\left(\frac{1}{36}\begin{pmatrix}u^3\\ u^2\\ u^1\\ 1\end{pmatrix}^T \mathbf{M}_\alpha \begin{bmatrix}\log(\mathbf{D}_{0,0}) & \log(\mathbf{D}_{0,1}) & \log(\mathbf{D}_{0,2}) & \log(\mathbf{D}_{0,3})\\ \log(\mathbf{D}_{1,0}) & \log(\mathbf{D}_{1,1}) & \log(\mathbf{D}_{1,2}) & \log(\mathbf{D}_{1,3})\\ \log(\mathbf{D}_{2,0}) & \log(\mathbf{D}_{2,1}) & \log(\mathbf{D}_{2,2}) & \log(\mathbf{D}_{2,3})\\ \log(\mathbf{D}_{3,0}) & \log(\mathbf{D}_{3,1}) & \log(\mathbf{D}_{3,2}) & \log(\mathbf{D}_{3,3})\end{bmatrix} \mathbf{M}_\alpha^T \begin{pmatrix}v^3\\ v^2\\ v^1\\ 1\end{pmatrix}\right) \tag{4}$$

For the interlayer interpolation of DTI, cubic B-spline curve equations in Log-Euclidean space for DTI interpolation and the interpolated tensor can be obtained by interpolating the four surrounding tensors. For the layer interpolation of DTI, cubic B-spline surface equations in Log-Euclidean space for DTI interpolation and the interpolated tensor can be obtained by the interpolation of the 16 surrounding tensors. Because of the high order continuity of the B-spline, this method can process the tensor image with noise, and the interpolation image is smooth.

2.4. Registration of DTI and T1 MRI

T1 images are scalar images, while DTI images are tensor images. Registration of different modal images is complex. DTI derivative images are scalar images, so they can be selected for registration with T1 MRI. However, the registration results between different DTI derivative images and T1 MRI are normally different. It is still a open question on which DTI derivative image is the best for the registration of DTI and T1 images. Fractional Anisotropy (referred to as FA) image, Mean Diffusion (referred to as MD) image, and b0 image is derived from DTI are chosen for DTI and T1 MRI registration in this paper. In the MD image and b0 image, cerebrospinal fluid show a high signal and white color, which is the opposite of T1 MRI. Therefore, the MD image and b0 image are processed by inverse gray transformation, named MD-inverse (referred to as MD-in) image and b0-inverse (referred to as b0-in) image, which makes cerebrospinal fluid shows low signal and gray color. After this processing, the MD-in image and b0-in image are similar to T1 MRI, so that they can be used for DTI and T1 MRI registration.

We use multi-modality medical image registration-based DTI derivative images for the registration of DTI and T1 MRI. Speciifically, syn registration algorithm is used for registration, where five kinds of DTI derivative images are used. Visual evaluation, the overlap and error rates after registration were used to evaluate the results. Since the punctate lesion of PWMD is located on the T1 image, the location of the lesion needs to be accurate and cannot be changed. Therefore, in this paper, the T1 image is used as the template to register DTI on the T1 image to obtain the registered DTI image. The experimental procedure of the registration part is shown in Fig.2.

2.4.1. T1 MRI mask making

DTI mask can be generated automatically during DTI preprocessing. However, the neonatal brain is not fully developed, and there is no apparent separation between the brain tissue and the skull. In addition, the artifact of neonatal data collection is significant, resulting in the mask's low accuracy generated by neonatal T1 MRI. To generate a more accurate T1 MRI mask, T1 MRI was selected as the template to register the b0 image, and the generated deformation field was applied to the DTI mask to obtain a more accurate T1 MRI mask. This T1 MRI mask can be used as input in registration. Fig.3 shows the mask of two images.

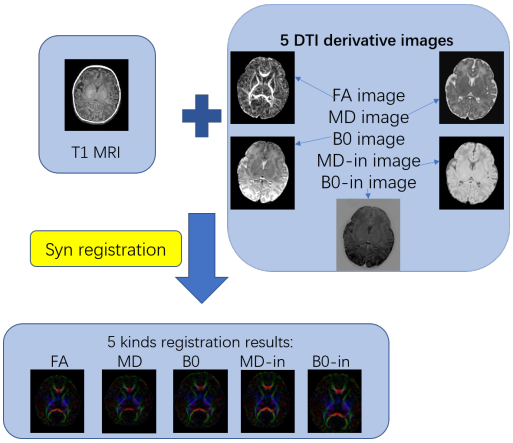

Figure 2: Syn registration algorithm and DTI derivative images.

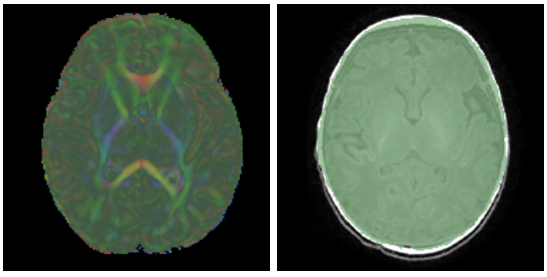

Figure 3: Left is the DTI mask generated automatically; right is the T1 MRI mask generated manually.

2.4.2. Registration results and evaluation

The registration results of DTI and T1 MRI are shown in Fig.4. From b0 image and FA image registration results, it can be seen that genu is almost invisible on the same slice. For MD image, MD-in image, and b0-in image registration results, genu is clearer on the same slice. Therefore, it can be speculated that the registration results of the MD image, MD-in image, and b0-in image is better than that of the b0 image and FA image, among which the FA image has the worst registration effect.

Many subjective factors in the visual evaluation results might be prone to unpredictable errors and may lead to inaccurate evaluation results.

However, the object in this study is neonatal with suspected PWMD, so the registration data selected are all neonatal. Because neonatal brain development is incomplete, and the white matter fiber bundle is thin and not completely myelin, most of the multi-modality image registration evaluation criteria only apply to adult DTI data. Therefore, in this paper, the overlapping rate and error rate Forsberg et al. (2011) of the brain tissue of the registered DTI and T1 images were selected to evaluate the results of multi-modality image registration.

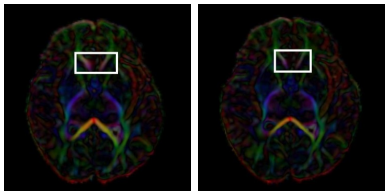

(a) b0 registration result (b) FA registration result

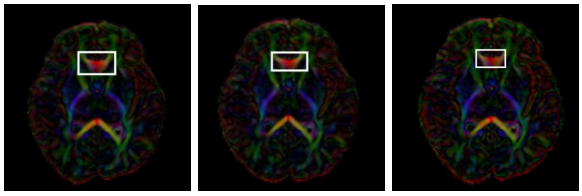

(c) MD registration result (d) b0-in registration result (e) MD-in registration result

Figure 4: Different registration results with Syn algorithm in the same slice; the white box is the region of genu.

We selected two overlapping rates to evaluate the overall brain registration accuracy of multi-modality image registration. The quantitative indexes measure expressed as the degree of overlap between the template image and the image volume after registration. The first quantitative index is Template Overlap (referred to as TO), which is defined as the volume of the overlapping region of the template image and the registered image divided by the volume of the template image. The larger the TO is, the better the registration result will be. TO is given by

$$TO = \frac{Tem \bigcap Mov}{Tem} \tag{5}$$

Tem represents the template image region which means T1 MRI. Mov is the image volume after registration which means registered DTI. $Tem \bigcap Mov$ represents the area of the overlapping area between the template image and the image after registration.

The second quantitative index is Union Overlap (referred to as UO), defined as the overlapping area volume of the template image and the registered image divided by the area volume of the template image and the registered image union. The larger the UO is, the better the registration result will be. UO is given by

$$UO = \frac{Tem \bigcap Mov}{Tem \bigcup Mov} \tag{6}$$

To supplement the evaluation criteria in the above equations, false-negative errors (referred to as FNE) and False positive errors (FPE) are also calculated. FNE is a measure of the template image volume incorrectly identified as a non-template image in registration. It is the volume of the template image outside the registered image divided by the volume of the template image. The smaller the UO is, the better the registration result will be. FNE is given by

Table 1
Average of four parameters.

	FA	MD	MD-in	b0	b0-in
TO	0.8716	0.9178	0.9300	0.8955	0.9315
UO	0.8284	0.8400	0.8409	0.8296	0.8499
FNE	0.1063	0.0617	0.0694	0.0736	0.0635
FPR	0.1052	0.1220	0.1184	0.1232	0.0945

$$FNE = \frac{Tem \backslash Mov}{Tem} \tag{7}$$

$Tem \backslash Mov$ represents the size of the part of the template image that does not overlap with the registered image.

FPE is a measure of the volume outside the template image that has been incorrectly identified as a template image which is defined as the volume outside the template image divided by the volume of the registered image, which is given by

$$FPE = \frac{Mov \backslash Tem}{Mov} \tag{8}$$

$Mov \backslash Tem$ represents the size of the part of the image that does not overlap with the template image after registration.

We use 5 DTI-derived images and Syn registration algorithms to register six newborn subjects. And the TO, UO, FNE, and FPE of registration results are averaged to evaluate the registration result as shown in Table 1.

From the results, we can see the following:

For all of the DTI-derived images, the comparisons are

$$TO_{b0-in} > TO_{MD-in} > TO_{MD} > TO_{b0} > TO_{FA}$$
$$UO_{b0-in} > UO_{MD-in} > UO_{MD} > UO_{b0} > UO_{FA}$$
$$FNE_{MD} < FNE_{b0-in} < FNE_{MD-in} < FNE_{b0} < FNE_{FA}$$
$$FPE_{b0-in} < FPE_{FA} < FPE_{MD-in} < FPE_{MD} < FPE_{b0}$$

The best result is the b0-in image, and the result of the MD-in image is a little worse than the b0-in image. The result of the MD image is third, and the result of the b0 and FA image is the worst, consistent with the visual evaluation.

2.5. Draw 15 ROIs

There are about 15 ROIs associated with PWMD, namely Genu, Splenium, bilateral cingulum (referred to as cg), bilateral corticospinal tract (referred to as cst), bilateral superior thalamic radiation (referred to as str), bilateral posterior thalamic radiation (referred to as ptr), superior bilateral fasciculi fronto-occipitalis (referred to as sfo) and brain fornix (referred to as fx). We have drawn these 15 ROIs in DTI, as shown in Fig. 5.

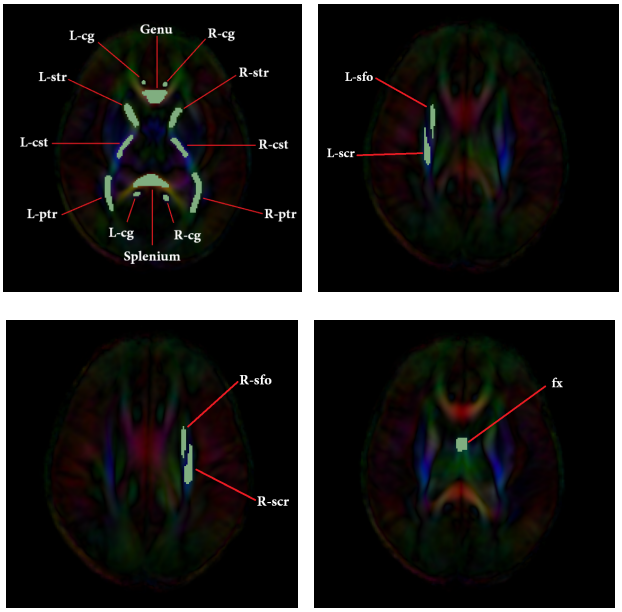

Figure 5: Neonatal DTI with 15 ROIs. The green part is the marked ROIs, and the names of ROIs are marked with red lines and white words.

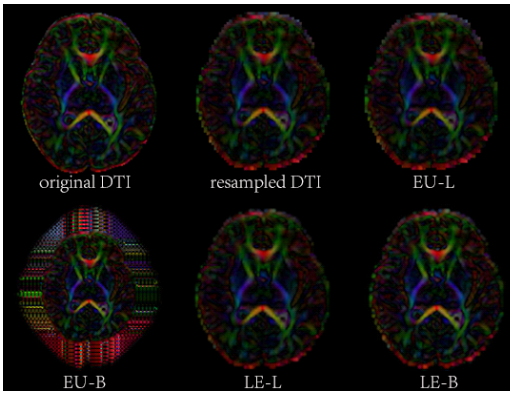

Figure 6: Four interpolation results for Linear interpolation based on Euclidean space (EU-L), B-spline interpolation based on Euclidean space (EU-B), Linear interpolation based on Log-Euclidean space (LE-L) and B-spline interpolation based on Log-Euclidean space (LE-B).

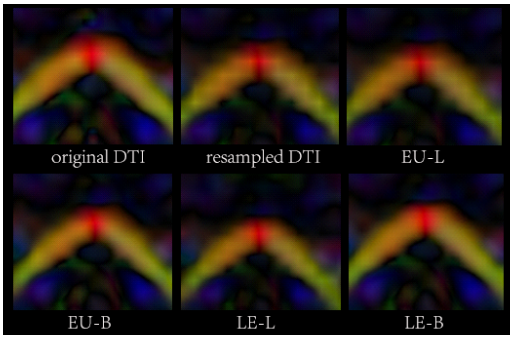

Figure 7: Genu in four interpolated DTI. The first one is original DTI, The second one is resample DTI, The last four pictures show four different interpolation results.

3. Results

3.1. DTI super-resolution

To compare the difference between original DTI and interpolated DTI to evaluate the effect of the interpolation method, the original DTI with resolution of 256×256×44, is resampled to obtain the DTI with resolution of 128×128×30 firstly. And then, the resampled DTI is interpolated by a different tensor interpolation method to obtain the new DTI, of which resolution is restored to 256×256×44. The resolution of both original DTI and interpolated DTI are 256×256×44, so they can be compared to evaluate different tensor interpolation methods. The interpolated results of the four methods are shown in Fig.7.

It can be seen from Fig.6, the DTI edge becomes rough after the down-sampling, and each part is jagged due to the reduction of resolution. Four different interpolation methods were used to interpolate the DTI after the reduction of sampling. The DTI edge of EU-L DTI is fuzzy and jagged. In EU-B DTI, a series of error interpolation tensor points appear outside DTI, but the other part is smooth. In LE-L DTI, the interpolated edge is smoother, but each part still has some serration. In LE-B DTI, the interpolated edge and each part in DTI are relatively smooth, and there is no problem with many false interpolation tensor points in EU-B. Therefore, the effect of the B-spline interpolation method based on Log-Euclidean space is the best.

The genu in interpolated DTI was magnified for observation, as shown in Fig.7.

It can be seen from Fig.7, the genu of down-sampling DTI becomes fuzzy and jagged. The Genu in EU-L and LE-L DTI are still relatively fuzzy, and the optimization effect of interpolation is very low compared with the down-sampling DTI. The Genu in EU-B and LE-B DTI are relatively clear and smooth, which is very close to genu in original DTI. Therefore, the effect of the B-spline interpolation method based on Log-Euclidean space is the best.

The DTI fiber tractography results in different ROIs are the focus of this paper, so the fiber tractography results of genu, splenium, str and ptr before and after interpolation in 6 subjects are selected. The average FA values of 6 subjects of DTI fiber tractography results are calculated, and shown in Table.2.

It can be seen from Table.5, the FA values of DTI fiber tractography results of EU-L and LE-L are significantly decreased. The FA values of DTI fiber tractography results of EU-B and LE-B decrease less, and LE-B is closest to the original data. Therefore, the anisotropy of interpolated DTI is well maintained with LE-B.

Three kinds of DTI derivative images, FA image, Mode image and RA image, are chosen to analyze the derivative images of interpolated DTI and original DTI by MSE. MSE represents the mean of the sum of squares of errors at the

Table 2
The average FA values of interpolated DTI fiber tractography.

	splenium	genu	str	ptr
original	0.4399	0.3643	0.2597	0.3098
EU-L	0.3709	0.3053	0.2224	0.2734
EU-B	0.4231	0.3400	0.2481	0.2965
LE-L	0.3838	0.3094	0.2229	0.2750
LE-B	0.4267	0.3401	0.2490	0.3006

Table 3
MSE comparison of interpolated DTI and original DTI.

	FA	Mode	RA
EU-L	0.0054	0.0546	0.0015
EU-B	0.0447	0.0674	0.0290
LE-L	0.0036	0.0481	0.0084
LE-B	0.0035	0.0420	0.0072

corresponding points between the interpolated DTI and the original DTI. The result is shown in Table 3.

The smaller is the MSE, the smaller the difference between the interpolated DTI and the original DTI will be. It can be seen from Table 6, the interpolated result of LE-B is the best, and the interpolated result of EU-L and EU-B is the worst.

The above interpolation operation is to interpolate the down-sampling DTI to the same resolution as the original DTI. The only purpose is to evaluate and analyze the interpolation algorithm by comparing the difference between the original DTI and the interpolated DTI, and the conclusion is that B-spline tensor interpolation based on Log-Euclidean space is the best. However, this paper aims to interpolate the original DTI to the same resolution as T1 MRI. After interpolation, the DTI resolution is greatly improved, and the fiber tractography results are optimized. The resolution of T1 MRI is 256×256×108, and the resolution of original DTI is 256×256×44. Its resolution is low, and the fiber tractography result is poor. After the above analysis, the B-spline interpolation method based on Log-Euclidean space is selected to interpolate the original DTI, and the resolution of interpolated DTI is increased to 256×256×108.

Splenium, Genu, str and ptr are selected as examples. The fiber tractography results of original DTI and interpolated DTI are used to compare the changes before. The fiber tractography results of healthy adults were provided as a reference. The results are shown in Fig.8.

It can be seen that the fiber tractography results of DTI interpolated by B-spline interpolation method based on Log-Euclidean space have been optimized, which is closed to the fiber tractography results of DTI adult, especially Splenium and ptr.

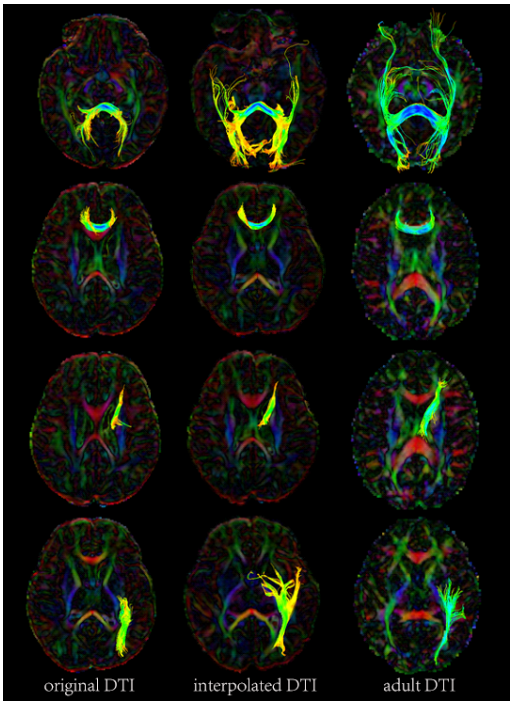

Figure 8: The fiber tractography results of original DTI, interpolated DTI, and adult DTI. The images from top to bottom are Genu, Splenium, str, ptr, and after interpolation.

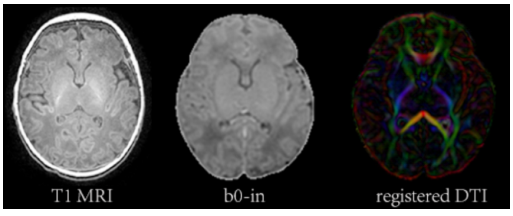

Figure 9: Registration results. The left two pictures show the T1 MRI and b0-in used in the registration process, and the third picture shows the registration results.

3.2. Registration of DTI and T1 MRI

The Syn registration method is selected. T1 MRI is taken as a template image, and a T1 mask is selected. The b0-in image was used for registration. The deformation field is applied to the original DTI, and the tensor orientation is conducted to obtain the final registered DTI. The results are shown in Fig.9. From left to right: T1 MRI, b0-in, and the final registered DTI.

3.3. Neonatal PWMD analysis

3.3.1. T1MRI lesion model construction

In the case of a neonatal T1, MRI suspected to have PWMD is shown in Fig.10. The lesions on T1 MRI are sketched manually, and the three-dimensional model of the lesions is constructed, as shown in Fig.11. For the convenience of analysis and observation, the 3D model of the lesion can be divided into six parts for analysis as shown

Table 4
The average FA values of interpolated DTI fiber tractography.

	a	b	c	d	e	f
slice	69-70	71-72	71-72	72-74	73-79	73-76
lesion superficial area(mm^2)	17.80	16.87	21.56	30.74	126.0	7.87
lesion volume(mm^3)	6.13	5.49	7.53	13.57	65.93	1.51

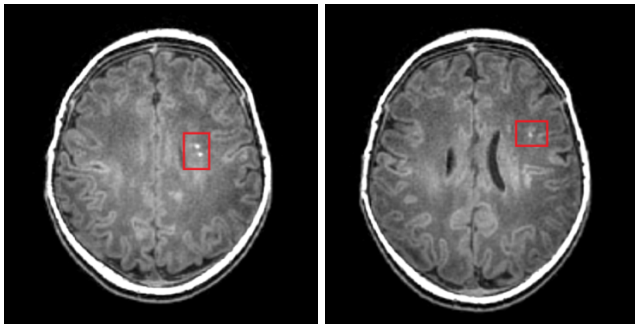

(a) (b)

Figure 10: Lesions in neonatal T1 MRI. The lesions are in a red rectangle which is very clear.

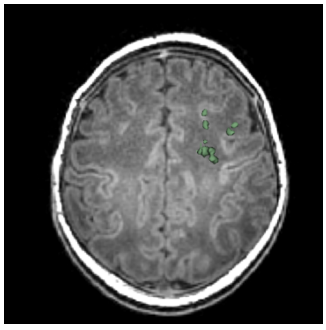

Figure 11: 3D model of lesions. The lesions area is marked with green.

in Fig.12. The 3D model of the lesion was analyzed with the results shown in Table 4.

3.3.2. Fiber tractography results and PWMD analysis

The DTI (interpolated and registered data previously) and generated 15 ROIs are used for fiber tractography. In addition, the fiber tractography is combined with the 3D lesion model generated above, and the position relationship is observed and analyzed, as shown in Fig.13.

It can be seen that the fiber tractography of r-ptr, r-sfo, r-scr, r-cst and r-str in the are close to the lesion model, where r-scr, r-sfo and r-cst intersect with the lesion. The degree of fiber tract damage with PWMD can be estimated from the proportion of fiber tracts affected by the PWMD lesion model to total fiber tracts e, and the results are shown in Table 5.

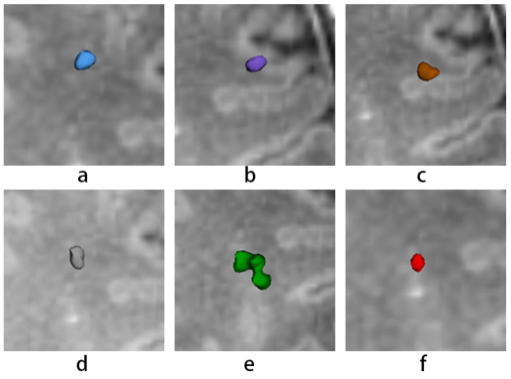

Figure 12: Six parts of the 3D lesion model. In each image, we mark the lesion area with different colors to distinguish it from the surrounding grayscale image.

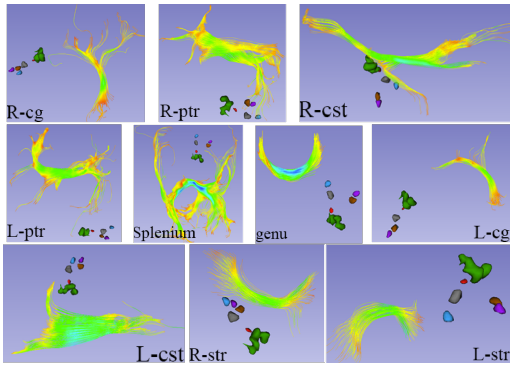

Figure 13: Combine 3D lesion model with fiber tractography. The yellow green lines in the figure represent fiber bundles, and the irregular spheres in other colors represent lesions.

Table 5
The damage degree of fiber tracts.

	total	damaged fiber tracts	damage degree
R-sfo	9	4	44.4%
R-scr	107	12	11.21%
R-cst	267	9	3.37%

This paper proposes a new technique of neonatal PWMD analysis based on DTI interpolation and multi-modality image registration. The algorithm includes B-spline interpolation based on Log-Euclidean space, multi-modality image registration of DTI and T1 MRI, and analysis of the influence of PWMD lesion on fiber tracts. DTI super-resolution and

multi-modality registration algorithms are effective and can predict and analyze PWMD.

Punctate White Matter Damage (PWMD) is one of the most common white matter damages. Therefore, converting undetectable clinical symptoms into quantifiable results to analyze and predict PWMD using related medical image processing methods is crucial for disease treatment, neurodevelopment, and possible future methods.

Because the acquisition of neonatal DTI is complex, the resolution is much lower than T1 MRI, which is not conducive to the registration of T1 images, and the development of neonatal white matter fiber tracts is not complete; the obtained results of fiber tractography are poor. To solve this problem, the super-resolution method can be adopted for neonatal DTI to improve the resolution of DTI, facilitate the realization of registration, and help improve the results of DTI fiber tractography. In addition, T1 images need to be registered with DTI to fuse the lesions in T1 images with the white matter fiber tracts of DTI; while DTI is a tensor image and T1 images are scalar images, the registration is complex because the DTI has a variety of scalar derivative images that can be used with T1 image registration.

Therefore, this paper proposes a new method to analyze neonatal white matter injury based on DTI interpolation and multi-mode image registration. In this paper, a b-spline interpolation method based on Log-Euclidean space is implemented to interpolate neonatal DTI, and the three times B-spline interpolation method of Euclidean space is applied to Log-Euclidean space, which is suitable for tensor calculation. The interpolation method ensures the essential characteristics of the tensor, avoids the swelling effect and non-positive definite effect of the interpolation tensor, and improves the tensor information of the neonatal DTI, making the results of fiber tractography richer and more accurate.

Subsequently, Syn registration method was used to register five derivative images of DTI (FA, MD, b0, md-in, and b0-in image). The evaluation indexes based on vision and overlap rate were selected to evaluate the registration results. The results showed that the b0-in image had the best effect. Finally, the T1 MRI lesions were 3D modeled, and the neonatal DTI containing 15 ROIs was made and used for DTI fiber tractography.

By mapping the results of fiber tractography with the lesion model in the same space, the parameters of the lesion model and the degree of influence on the fiber tracts were calculated. And the damage situation of neonatal PWMD was analyzed, which can effectively provide references for the diagnosis and prediction of PWMD.

In the experiment, it was found that some essential fiber tracts of the neonatal were not myelin sheathing and could not be displayed by interpolation (such as slf), making the experimental results imperfect. Regarding registration, the effect of using the T2 image as the medium to register the T1 image with DTI should be the best. However, there is no T2 image in the data, so the registration result needs improvement. Overall, according to the existing data and actual situation, the method in the paper can provide practical help for the early analysis of neonatal PWMD.

4. Discussion

This paper proposes a new technique of neonatal PWMD analysis based on DTI interpolation and multi-modality image registration. The algorithm includes B-spline interpolation based on Log-Euclidean space, multi-modality image registration of DTI and T1 MRI, and analysis of the influence of PWMD lesion on fiber tracts. DTI super-resolution and multi-modality registration algorithms are effective and can predict and analyze PWMD.

Punctate White Matter Damage (PWMD) is one of the most common white matter damages. Therefore, converting undetectable clinical symptoms into quantifiable results to analyze and predict PWMD using related medical image processing methods is crucial for disease treatment, neurodevelopment, and possible future methods.

Because the acquisition of neonatal DTI is complex, the resolution is much lower than T1 MRI, which is not conducive to the registration of T1 images, and the development of neonatal white matter fiber tracts is not complete; the obtained results of fiber tractography are poor. To solve this problem, the super-resolution method can be adopted for neonatal DTI to improve the resolution of DTI, facilitate the realization of registration, and help improve the results of DTI fiber tractography. In addition, T1 images need to be registered with DTI to fuse the lesions in T1 images with the white matter fiber tracts of DTI; while DTI is a tensor image and T1 images are scalar images, the registration is complex because the DTI has a variety of scalar derivative images that can be used with T1 image registration.

Therefore, this paper proposes a new method to analyze neonatal white matter injury based on DTI interpolation and multi-mode image registration. In this paper, a b-spline interpolation method based on Log-Euclidean space is implemented to interpolate neonatal DTI, and the three times B-spline interpolation method of Euclidean space is applied to Log-Euclidean space, which is suitable for tensor calculation. The interpolation method ensures the essential characteristics of the tensor, avoids the swelling effect and non-positive definite effect of the interpolation tensor, and improves the tensor information of the neonatal DTI, making the results of fiber tractography richer and more accurate.

Subsequently, Syn registration method was used to register five derivative images of DTI (FA, MD, b0, md-in, and b0-in image). The evaluation indexes based on vision and overlap rate were selected to evaluate the registration results. The results showed that the b0-in image had the best effect. Finally, the T1 MRI lesions were 3D modeled, and the neonatal DTI containing 15 ROIs was made and used for DTI fiber tractography.

By mapping the results of fiber tractography with the lesion model in the same space, the parameters of the lesion model and the degree of influence on the fiber tracts were calculated. And the damage situation of neonatal PWMD

was analyzed, which can effectively provide s for the diagnosis and prediction of PWMD.

In the experiment, it was found that some essential fiber tracts of the neonatal were not myelin sheathing and could not be displayed by interpolation (such as slf), making the experimental results imperfect. Regarding registration, the effect of using the T2 image as the medium to register the T1 image with DTI should be the best. However, there is no T2 image in the data, so the registration result needs improvement. Overall, according to the existing data and actual situation, the method in the paper can provide practical help for the early analysis of neonatal PWMD.

5. Conclusions and Future Directions

This paper proposes a new technique of neonatal PWMD analysis based on DTI interpolation and multi-modality image registration. The three times B-spline interpolation based on the Log-Euclidean space is used for neonatal DTI interpolation, improving its resolution and facilitating fiber tractography. Syn registration algorithms and five DTI derivative images (FA, MD, b0, MD-in, and b0-in image) were selected for multi-modality image registration of DTI and T1 MRI. The results show that the b0-in images are the best. The DTI and T1 MRI were registered using this method, 3D lesions model on T1 MRI was made, and the neonatal DTI with 15 ROIs was built for individual DTI fiber tractography results. The 3D lesion model was combined with fiber tractography results to analyze and predict the degree of PWMD lesion affecting fiber tracts. This method plays an essential auxiliary role in diagnosing and treating neonatal PWMD. Because there is too little data in this paper to use deep learning, a large number of data sets can be collected in the future, and the method of deep learning can be used as a further research method.

Acknowledgments

This work was supported by the National Natural Science Foundation of China (62071384), the Key Research and Development Project of Shaanxi Province of China (2023-YBGY-239), Natural Science Basic Research Plan in Shaanxi Province of China (2023-JC-YB-531).

References

Arrigoni, F., Peruzzo, D., Gagliardi, C., Maghini, C., Colombo, P., Iammarrone, F. S., Pierpaoli, C., Triulzi, F., & Turconi, A. C. (2016). Whole-brain dti assessment of white matter damage in children with bilateral cerebral palsy: evidence of involvement beyond the primary target of the anoxic insult. *American Journal of Neuroradiology*, *37*, 1347–1353.

Arsigny, V. (2004). *Processing data in lie groups: An algebraic approach. Application to non-linear registration and diffusion tensor MRI*. Ph.D. thesis Citeseer.

Arsigny, V., Fillard, P., Pennec, X., & Ayache, N. (2006). Log-euclidean metrics for fast and simple calculus on diffusion tensors. *Magnetic Resonance in Medicine: An Official Journal of the International Society for Magnetic Resonance in Medicine*, *56*, 411–421.

Avants, B., Duda, J. T., Zhang, H., & Gee, J. C. (2007). Multivariate normalization with symmetric diffeomorphisms for multivariate studies. In *International Conference on Medical Image Computing and Computer-Assisted Intervention* (pp. 359–366). Springer.

B, L. Z. (2007). Research on enhancement and interpolation algorithms in medical image processing(in chinese).

Barmpoutis, A., Vemuri, B. C., Shepherd, T. M., & Forder, J. R. (2007). Tensor splines for interpolation and approximation of dt-mri with applications to segmentation of isolated rat hippocampi. *IEEE transactions on medical imaging*, *26*, 1537–1546.

Bashir, S. M. A., & Wang, Y. (2021a). Deep learning for the assisted diagnosis of movement disorders, including isolated dystonia. *Frontiers in Neurology*, (p. 668).

Bashir, S. M. A., & Wang, Y. (2021b). Small object detection in remote sensing images with residual feature aggregation-based super-resolution and object detector network. *Remote Sensing*, *13*, 1854.

Bashir, S. M. A., Wang, Y., Khan, M., & Niu, Y. (2021). A comprehensive review of deep learning-based single image super-resolution. *PeerJ Computer Science*, *7*, e621.

Dong, C., Loy, C. C., He, K., & Tang, X. (2014). Learning a deep convolutional network for image super-resolution. In *European conference on computer vision* (pp. 184–199). Springer.

Fillard, P. (2008). *Riemannian processing of tensors for diffusion MRI and computational anatomy of the brain.*. Ph.D. thesis Université Nice Sophia Antipolis.

Forsberg, D., Rathi, Y., Bouix, S., Wassermann, D., Knutsson, H., & Westin, C.-F. (2011). Improving registration using multi-channel diffeomorphic demons combined with certainty maps. In *International Workshop on Multimodal Brain Image Analysis* (pp. 19–26). Springer.

Haris, M., Shakhnarovich, G., & Ukita, N. (2018). Deep back-projection networks for super-resolution. In *Proceedings of the IEEE conference on computer vision and pattern recognition* (pp. 1664–1673).

Hotz, I., Sreevalsan-Nair, J., Hagen, H., & Hamann, B. (2010). Tensor field reconstruction based on eigenvector and eigenvalue interpolation. In *Dagstuhl Follow-Ups*. Schloss Dagstuhl-Leibniz-Zentrum fuer Informatik volume 1.

Kung, G. L., Nguyen, T. C., Itoh, A., Skare, S., Ingels Jr, N. B., Miller, D. C., & Ennis, D. B. (2011). The presence of two local myocardial sheet populations confirmed by diffusion tensor mri and histological validation. *Journal of Magnetic Resonance Imaging*, *34*, 1080–1091.

Ledig, C., Theis, L., Huszár, F., Caballero, J., Cunningham, A., Acosta, A., Aitken, A., Tejani, A., Totz, J., Wang, Z. et al. (2017). Photo-realistic single image super-resolution using a generative adversarial network. In *Proceedings of the IEEE conference on computer vision and pattern recognition* (pp. 4681–4690).

Lim, B., Son, S., Kim, H., Nah, S., & Mu Lee, K. (2017). Enhanced deep residual networks for single image super-resolution. In *Proceedings of the IEEE conference on computer vision and pattern recognition workshops* (pp. 136–144).

Miller, M. I., Beg, M. F., Ceritoglu, C., & Stark, C. (2005). Increasing the power of functional maps of the medial temporal lobe by using large deformation diffeomorphic metric mapping. *Proceedings of the National Academy of Sciences*, *102*, 9685–9690.

Nguyen, A. L., Ding, Y., Suffren, S., Londono, I., Luck, D., & Lodygensky, G. A. (2019). The brains kryptonite: overview of punctate white matter lesions in neonates. *International Journal of Developmental Neuroscience*, *77*, 77–88.

Niwa, T., de Vries, L. S., Benders, M. J., Takahara, T., Nikkels, P. G., & Groenendaal, F. (2011). Punctate white matter lesions in infants: new insights using susceptibility-weighted imaging. *Neuroradiology*, *53*, 669–679.

Pennec, X., Fillard, P., & Ayache, N. (2006). A riemannian framework for tensor computing. *International Journal of computer vision*, *66*, 41–66.

Sloan, J. M., Goatman, K. A., & Siebert, J. P. (2018). Learning rigid image registration-utilizing convolutional neural networks for medical image registration, .

Studholme, C. (2007). Incorporating dti data as a constraint in deformation tensor morphometry between t1 mr images. In *Biennial International Conference on Information Processing in Medical Imaging* (pp. 223–232). Springer.

Tang, C., Xie, X., & Du, R. (2013). Multi-modal image registration based on diffeomorphic demons algorithm. In *Fifth International Conference on Digital Image Processing (ICDIP 2013)* (pp. 309–313). SPIE volume 8878.

Tusor, N., Benders, M. J., Counsell, S. J., Nongena, P., Ederies, M. A., Falconer, S., Chew, A., Gonzalez-Cinca, N., Hajnal, J. V., Gangadharan, S. et al. (2017). Punctate white matter lesions associated with altered brain development and adverse motor outcome in preterm infants. *Scientific reports*, *7*, 1–9.

Wang, Y., Bashir, S. M. A., Khan, M., Ullah, Q., Wang, R., Song, Y., Guo, Z., & Niu, Y. (2022). Remote sensing image super-resolution and object detection: Benchmark and state of the art. *Expert Systems with Applications*, (p. 116793).

Wang, Y.-J., & Mao, J. (2014). Types of acute hypoxic-ischemic brain injury due to perinatal sentinel events in neonates. *Zhongguo Dang dai er ke za zhi= Chinese Journal of Contemporary Pediatrics*, *16*, 589–595.

Yassine, I. A. (2010). High rank tensor and spherical harmonic models for diffusion mri processing, .

Zhukov, L., & Barr, A. H. (2002). Oriented tensor reconstruction: Tracing neural pathways from diffusion tensor mri. In *IEEE Visualization, 2002. VIS 2002.* (pp. 387–394). IEEE.